

## Research Submission

# Migraine Subclassification via a Data-Driven Automated Approach Using Multimodality Factor Mixture Modeling of Brain Structure Measurements

Todd J. Schwedt, MD; Bing Si, MS; Jing Li, PhD; Teresa Wu, PhD; Catherine D. Chong, PhD

**Background.**—The current subclassification of migraine is according to headache frequency and aura status. The variability in migraine symptoms, disease course, and response to treatment suggest the presence of additional heterogeneity or subclasses within migraine.

**Objective.**—The study objective was to subclassify migraine via a data-driven approach, identifying latent factors by jointly exploiting multiple sets of brain structural features obtained via magnetic resonance imaging (MRI).

**Methods.**—Migraineurs ( $n = 66$ ) and healthy controls ( $n = 54$ ) had brain MRI measurements of cortical thickness, cortical surface area, and volumes for 68 regions. A multimodality factor mixture model was used to subclassify MRIs and to determine the brain structural factors that most contributed to the subclassification. Clinical characteristics of subjects in each subgroup were compared.

**Results.**—Automated MRI classification divided the subjects into two subgroups. Migraineurs in subgroup #1 had more severe allodynia symptoms during migraines ( $6.1 \pm 5.3$  vs.  $3.6 \pm 3.2$ ,  $P = .03$ ), more years with migraine ( $19.2 \pm 11.3$  years vs  $13 \pm 8.3$  years,  $P = .01$ ), and higher Migraine Disability Assessment (MIDAS) scores ( $25 \pm 22.9$  vs  $15.7 \pm 12.2$ ,  $P = .04$ ). There were not differences in headache frequency or migraine aura status between the two subgroups.

**Conclusions.**—Data-driven subclassification of brain MRIs based upon structural measurements identified two subgroups. Amongst migraineurs, the subgroups differed in allodynia symptom severity, years with migraine, and migraine-related disability. Since allodynia is associated with this imaging-based subclassification of migraine and prior publications suggest that allodynia impacts migraine treatment response and disease prognosis, future migraine diagnostic criteria could consider allodynia when defining migraine subgroups.

**Key words:** migraine, allodynia, magnetic resonance imaging, classification, cortical thickness, brain structure, headache, cortical surface area, brain volume, factor mixture model, multimodality factor mixture model

(*Headache* 2017;57:1051-1064)

## INTRODUCTION

The current subclassification structure for migraine is unlikely to represent the entire heterogeneity that

is present amongst the migraine population. According to the International Classification of Headache Disorders-3 beta (ICHD-3 beta), migraine is subclassified according to the presence or absence of aura and according to headache frequency (ie, episodic migraine vs chronic

---

From the Department of Neurology, Mayo Clinic, Phoenix, AZ (T.J. Schwedt and C.D. Chong); School of Computing, Informatics, and Decision Systems Engineering, Arizona State University, Phoenix, AZ, USA (B. Si, J. Li, and T. Wu).

Address all correspondence to T.J. Schwedt, Department of Neurology, Mayo Clinic, 5777 East Mayo Blvd, Phoenix, AZ 85054, USA, email: Schwedt.todd@mayo.edu

Accepted for publication April 10, 2017.

---

*Conflict of interest:* Within the last 12 months, Todd Schwedt: Consulting/Advisory Boards—Allergan, Amgen, Autonomic Technologies, Avanir, Dr. Reddy's, Nocira, Novartis; Options—Nocira, Second Opinion; Royalties—UpToDate.

*Funding:* NIH K23NS070891 to TJS.

migraine).<sup>1</sup> Subclassifying migraine according to aura status is justified due to the likelihood that there are underlying pathophysiologic differences between migraine with aura and migraine without aura attacks. Dividing people with migraine according to headache frequency is one way of estimating total headache burden, the likelihood of co-morbidities, and even the likelihood of treatment response in some cases (eg, onabotulinumtoxinA for chronic migraine only). Although this classification structure according to aura status and headache frequency accounts for some important migraine features, it omits others (eg, number of years with migraine, presence or absence of allodynia) that might also be important for migraine subclassification if they are associated with different pathophysiology, changes in brain structure or function, migraine prognosis, and treatment response.

Previously published studies have utilized brain imaging data to develop classification models for migraine, episodic migraine, and chronic migraine.<sup>2-4</sup> Those studies investigated the accuracy of imaging-based models for correctly identifying groups of subjects or individual subjects as having migraine versus being a healthy control or having episodic migraine versus chronic migraine. This study differs from prior investigations since the aim was to *identify migraine subgroups* based solely on brain imaging data, different from prior studies that aimed to accurately classify individuals into predefined groups. The objective of this study was to use a data-driven automated approach, using multimodality factor mixture modeling, to identify latent factors based upon MRI measurements including brain regional cortical thickness, surface area, and volume to subclassify people with migraine according to brain structure and then to explore whether there were differences in clinical features between patients in each of the subgroups. Healthy controls were included to determine if differences in brain structure lead to data-driven separation of migraine patients from healthy controls and to help with interpretation of study findings amongst the migraineurs. The overall goal was to use

migraine subclassification according to brain structure to identify clinical features that might be important when subclassifying migraine.

## METHODS

**Approvals and Consent.**—This study was approved by the Mayo Clinic Institutional Review Board and by the Washington University School of Medicine in St. Louis Institutional Review Board. Every subject underwent an informed consent process during which the potential risks and benefits of this study were explained and the subject provided written consent for their participation.

**Study Participants.**—Healthy controls without migraine and people with migraine were enrolled into this study. Participants were identified from the investigator's headache clinics, from a database of research volunteers, and from the communities surrounding the investigators' medical centers. Diagnoses of migraine were assigned using the diagnostic criteria of the International Classification of Headache Disorders 2 (ICHD-2).<sup>5</sup> Participants were free from: acute or chronic pain conditions other than migraine, contraindications to MRI, neurologic disorders other than migraine, daily medications that could be considered migraine prophylactic medications, opioid use, medication overuse (according to ICHD-2 criteria), and abnormal brain MRI scans according to usual clinical interpretation.

**Data Collection.**—Data collected from all participants included age, sex, medication use, medical history, Beck Depression Inventory-II (BDI-II) scores, State-Trait Anxiety Inventory (STAI) scores, hyperacusis scores via the Hyperacusis Questionnaire, photosensitivity scores via the Photosensitivity Assessment Questionnaire, and allodynia symptom severity between/without headaches using the Allodynia Symptom Checklist 12 (ASC-12).<sup>6-11</sup> Additional data collected from migraine participants included headache frequency, number of years with migraine, Migraine Disability Assessment (MIDAS) scores, allodynia symptom severity during migraine attacks using the ASC-12, and aura status.<sup>11,12</sup>

Participants were imaged on one of two Siemens (Erlangen, Germany) MRI machines, each at a different institution: (1) MAGNETOM Trio 3T

scanner using a 12-channel head matrix coil, or (2) MAGNETOM Skyra 3T scanner using a 20-channel head matrix coil. Structural scans included a high-resolution 3D T1-weighted sagittal magnetization prepared rapid gradient echo (MP-RAGE) series [Trio parameters: TE = 3.16 ms, TR = 2.4 s,  $1 \times 1 \times 1$  mm voxels, 256  $\times$  256 mm field of view (FOV), acquisition matrix 256  $\times$  256; Skyra parameters: TE = 3.03 ms; TR = 2.4 s;  $1 \times 1 \times 1.3$  mm voxels; 256  $\times$  256 mm FOV, acquisition matrix 256  $\times$  256] and T2-weighted images in axial plane (Trio parameters: TE = 88 ms, TR = 6280 ms,  $1 \times 1 \times 4$  mm voxels, 256  $\times$  256 mm FOV, acquisition matrix 256  $\times$  256; Skyra parameters: TE = 84 ms; TR = 6800 ms;  $1 \times 1 \times 4$  mm voxels; 256  $\times$  256 mm FOV, acquisition matrix 256  $\times$  256). Data obtained from T1 sequences were used for determining structural measures while T1 and T2 images were used for ruling out gross structural abnormalities. Nearly equal proportions of migraine and healthy control participants were imaged on each of the two MRI scanners: 32 of 54 (59%) healthy control participants were imaged on scanner one and 38 of 66 (58%) migraine participants were imaged on scanner one. Data included in this analysis have been utilized in prior analyses from our research group.<sup>3,4</sup>

T1 MP-RAGE sequence image processing was performed using the automated FreeSurfer image analysis suite (version 5.3, <http://surfer.nmr.mgh.harvard.edu/>). All image postprocessing was conducted using a single Mac workstation running OS X Lion 10.7.5 software, so as to prevent postprocessing irregularities derived from using multiple workstations.<sup>13</sup> FreeSurfer methodology is well described in prior papers.<sup>14</sup> Briefly, processing includes skull stripping, automated Talairach transformation, segmentation of subcortical gray and white matter, intensity normalization, and gray-white matter boundary tessellation and surface deformation.<sup>14-17</sup> This automatic segmentation and parcellation process provides information used to calculate regional cortical and subcortical volumes, cortical surface areas, and cortical thicknesses over the left and right hemispheres. For quality control, the automated segmentations and parcellations of each individual participant were manually inspected for errors before including

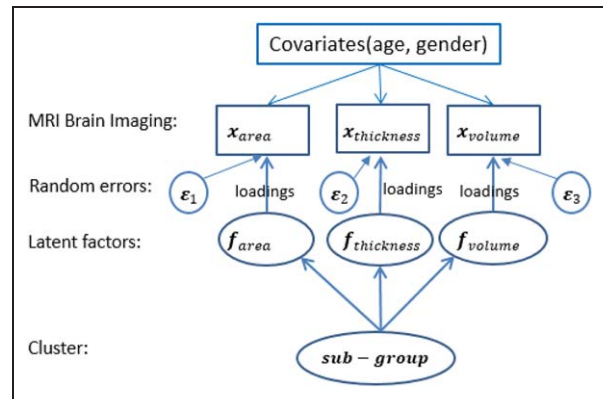


**Fig. 1.**—Path diagram of multimodality factor mixture model (MFMM). [Color figure can be viewed at [wileyonlinelibrary.com](http://wileyonlinelibrary.com)]

the data for statistical analysis. Mean thickness, surface area, and volume estimates were extracted from FreeSurfer and exported to MATLAB (2007a, MathWorks) for further analyses. Minimal manual correction was required for less than 5% of subjects. Since our analyses of study data demonstrated that there were not differences in clustering structure when utilizing right brain hemisphere regions and left brain hemisphere regions separately, structural measures were averaged over the right and left brain hemispheres so that there were 34 measures of cortical thickness, 34 measures of cortical surface area, and 34 measures of regional volume.

**Statistical Approach.**—Descriptive statistics were used to describe demographic data, scores on questionnaires, and headache characteristics. Two-tailed *t* tests or Fisher's exact tests were utilized for comparing these data between subject cohorts.

A factor mixture model (FMM) was used to subclassify the brain MRIs into subgroups.<sup>18</sup> A FMM assumes that there are latent factors underlying the observed features and that the latent factors are dependent on a latent multinomial variable that represents the unobserved subclassifications. The conventional FMM can only model a single set of features at a time. In our study, there are three sets of MRI features including cortical thickness, cortical surface area, and regional volumes. To model multiple sets of features, we used a multimodality FMM (MFMM). The key idea of MFMM is to use one FMM for each set of features and couple the

Table 1.—Participant Characteristics

	Migraine ( <i>n</i> = 66)	Healthy Controls ( <i>n</i> = 54)	<i>P</i> Value
Age in years (mean ± SD) ( <i>n</i> = 120)	36 ± 11	36.5 ± 11.2	.82
Sex (female:male) ( <i>n</i> = 120)	52:14	39:15	.53
State anxiety (mean ± SD) ( <i>n</i> = 120)	26.8 ± 7.1	24.8 ± 5.3	.08
Trait anxiety (mean ± SD) ( <i>n</i> = 120)	31.6 ± 8.9	28.8 ± 7.9	.08
Beck Depression Inventory (mean ± SD) ( <i>n</i> = 120)	4.1 ± 4.3	2.2 ± 4	.01*
Hyperacusis (mean ± SD) ( <i>n</i> = 114; data not available from 6 migraineurs)	8.6 ± 1.4	3.9 ± 3.5	<.001*
Photophobia (mean ± SD) ( <i>n</i> = 114; data not available from 6 migraineurs)	2.4 ± 2.5	1.0 ± 1.7	<.001*
Allodynia between/without headaches (mean ± SD) ( <i>n</i> = 120)	0.8 ± 0.4	0.1 ± 0.4	.01*
Headache days/month (mean ± SD) ( <i>n</i> = 66)	8.9 ± 6.2		
Years with migraine (mean ± SD) ( <i>n</i> = 66)	16.2 ± 10.4		
Migraine aura (yes/no) ( <i>n</i> = 60)	26/34		
MIDAS (mean ± SD) ( <i>n</i> = 66)	20.5 ± 19		
Allodynia during headache (mean ± SD) ( <i>n</i> = 66)	4.9 ± 1.6		

Migraine and healthy control subjects had similar age, sex, and anxiety scores. Although migraine participants had statistically higher depression scores, the mean depression scores amongst the migraine patients and the healthy control patients were both within “normal” or nondepressed ranges. As expected, migraine participants had higher scores for hyperacusis, photophobia, and allodynia. Anxiety scores were calculated from the State-Trait Anxiety Inventory. Allodynia scores during and between headaches were calculated from the Allodynia Symptom Checklist 12. Hyperacusis scores were calculated from the Hyperacusis Questionnaire. Photophobia scores were derived from the Photosensitivity Assessment Questionnaire. MIDAS = migraine disability assessment scale; SD = standard deviation.

FMMs by making their respective latent factors dependent on the same latent multinomial variable that represents the subclassifications; please see Figure 1 for the path diagram of the model. In this way, subclassifications are identified by jointly exploiting multiple sets of features rather than interrogating them in isolation.

As depicted in Figure 1, in the proposed MFMM, multimodality imaging features,  $\mathbf{x}_{\text{area}}$ ,  $\mathbf{x}_{\text{thickness}}$ , and  $\mathbf{x}_{\text{volume}}$ , are related to latent factors,  $f_{\text{area}}$ ,  $f_{\text{thickness}}$ , and  $f_{\text{volume}}$ , by modality-specific linear models. The latent factors are related to the subgroup variable by Gaussian mixture models. We also considered the potential influence of age and gender on imaging features and therefore added

age and gender as covariates in the MFMM. In Figure 1, observed variables are represented by rectangles. Latent variables are represented by ellipses/circles. Because this model includes latent variables, a typical method for estimating the model parameters is the expectation-maximization algorithm.

The detailed steps in applying the MFMM to our datasets are as follows: First, MFMM took as input three sets of data (ie, cortical thickness, cortical surface area, and regional volume features) for the same 120 subjects, and used an expectation-maximization algorithm to estimate the model coefficients.<sup>18</sup> This study has 120 samples, the size of which is comparable to some existing studies using FMM.<sup>19</sup> However, a larger sample size would be

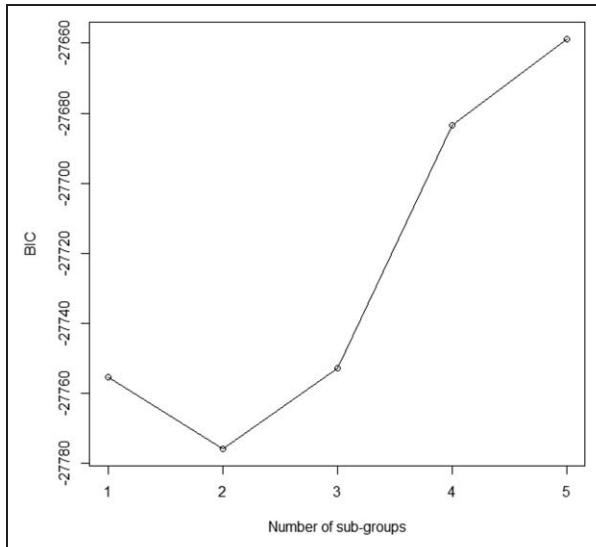


**Fig. 2.**—Bayesian information criterion (BIC) curve with number of subgroups from 1 to 5. [Color figure can be viewed at [wileyonlinelibrary.com](http://wileyonlinelibrary.com)]

beneficial for identifying more subtly different subgroups. The optimal number of subclassifications was identified using Bayesian information criterion (BIC).<sup>20</sup> Next, the estimated model coefficients allowed for computing a score that reflected the likelihood for an individual research subject MRI belonging to each of the subgroups. The research subject was assigned to the subgroup with the highest score. In this way, all the research subjects were classified. Finally, research subjects in different subgroups were compared by correlating their subgroup memberships with clinical variables including age, sex, headache frequency, number of years with migraine, aura status, allodynia symptom severity, migraine-related disability, hyperacusis severity, photophobia severity, anxiety scores, and depression scores.

## RESULTS

120 subjects were included in this study, consisting of 66 subjects with migraine and 54 healthy control subjects. Subject demographics, migraine characteristics, and scores of depression, anxiety, photophobia, hyperacusis, and allodynia are presented in Table 1. Overall, the average age of the subjects was 36.2 years and 75.8% were females. There were no differences in age or sex between

the migraine and healthy control cohorts. Average anxiety and depression scores amongst migraine participants and healthy control participants were within the nonanxious and nondepressed ranges. The migraine participants averaged 8.9 headache days per month, had migraine for an average of 16.2 years, and 43.3% had migraine aura. The average MIDAS score was 20.5, indicating moderate to severe migraine-related disability. Participants with migraine had higher photophobia, hyperacusis, and between headache/without headache allodynia scores compared to healthy controls.

Automated separation of the 120 subjects via MFMM of brain structural data divided the subjects into two subgroups. Figure 2 shows a BIC curve with different numbers of subgroups, which indicates a clear minimum at two subgroups.

The automated separation into two subgroups was based on seven MRI factors: two consisting of regional volume measurements, three consisting of cortical thickness measurements, and two consisting of cortical surface area measurements. These seven MRI factors and the individual contributions (ie, loadings) of specific brain regions to the factors and therefore to the subclassification of subjects into the two subgroups are demonstrated in Figure 3.

As shown in Tables 2–4, the majority of the significant MRI features shown in Figure 3 have significant mean differences between the two subgroups. Several MRI features do not have significant *P* values. This is because our clustering algorithm finds subgroups that differ in factors and the MRI features are linear combinations of the factors. Subgroup difference in the factors do not necessarily lead to subgroup difference in all the MRI features, although in most cases they do.

Subgroup #1 included 19 healthy controls and 34 subjects with migraine while subgroup #2 included 35 healthy controls and 32 subjects with migraine. Whereas the number of healthy controls in subgroup #1 significantly differed from the number in subgroup #2 ( $P = .002$ ), the number of subjects with migraine did not differ between the two subgroups.

Clinical characteristics of migraine subjects in subgroup #1 and subgroup #2 are shown in Table 5.

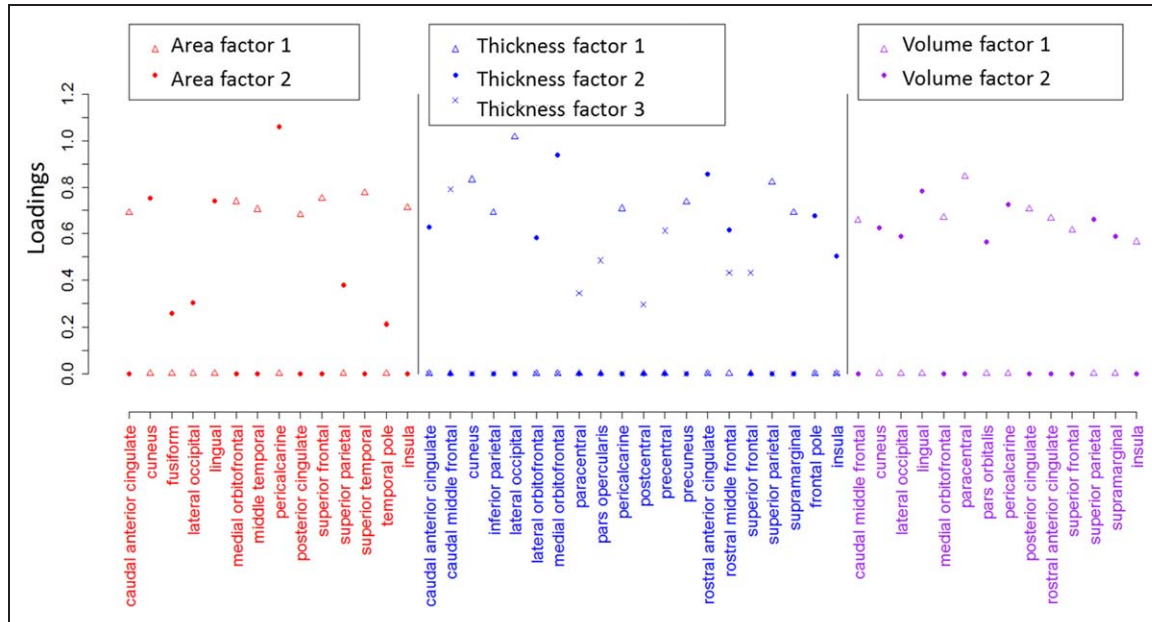


**Fig. 3.—Brain structure measurements that contributed to the data-driven subclassification of migraine. Measurements of brain cortical surface area, cortical thickness, and regional volumes significantly contributed to the automated subclassification of brain MRIs. Seven factors contributed to the model including: 2 factors composed of a combination of 14 surface area measures; 3 factors composed of a combination of 20 cortical thickness measures; and 2 factors composed of a combination of 14 volume measures. “Loading” is a measurement of how much an individual brain structural feature contributed to the classification. [Color figure can be viewed at wileyonlinelibrary.com]**

**Table 2.—Loadings on Significant Cortical Surface Area MRI Features and the Mean Surface Area Measurements for the Two Subgroups**

Regions for surface area	Loadings		Means of MRI features (mm <sup>2</sup> )		
	Factor 1	Factor 2	Subgroup 1	Subgroup 2	<i>P</i> value
Caudal anterior cingulate	0.690066	0	629.9434	736.5299	3.19E–08
Cuneus <sup>†</sup>	0	0.752737	1380.811	1486.142	0.004526
Fusiform	0	0.256507	3002.906	3296.627	7.15E–05
Lateral occipital <sup>†</sup>	0	0.301753	4248.783	4621.978	0.00061
Lingual	0	0.739706	2921.123	3119.03	0.005897
Medial orbitofrontal <sup>†</sup>	0.738162	0	1619.236	1836.642	4.14E–09
Middle temporal	0.704947	0	2895.66	3302.149	1.35E–07
Pericalcarine <sup>†</sup>	0	1.059257	1370.472	1426.627	0.173673
Posterior cingulate	0.682551	0	1078.283	1232.478	1.35E–07
Superior frontal <sup>†</sup>	0.751127	0	6287.472	7069.604	3.92E–08
Superior parietal <sup>†</sup>	0	0.378261	4963.255	5503.701	3.52E–06
Superior temporal	0.776636	0	3291.283	3715	2.81E–10
Temporal pole	0	0.210258	422.1415	448.4478	0.001073
Insula <sup>†</sup>	0.712146	0	1956.396	2188.194	1.14E–08

<sup>†</sup>Brain regions for which surface area, cortical thickness, and volume measurements of that region all contributed to subclassification.

**Table 3.—Loadings on Significant Cortical Thickness MRI Features and the Mean Cortical Thickness Measurements for the Two Subgroups**

Regions for Thickness	Loadings			Means of MRI Features (mm)		P Value
	Factor 1	Factor 2	Factor 3	Subgroup 1	Subgroup 2	
Caudal anterior cingulate	0	0.628274	0	2.603198	2.544045	0.14682
Caudal middle frontal	0	0	0.790955	2.406321	2.537396	1.12E-07
Cuneus†	0.83185	0	0	1.804151	1.845373	0.109452
Inferior parietal	0.691461	0	0	2.420425	2.507582	0.000169
Lateral occipital†	1.016006	0	0	2.185726	2.284821	0.000134
Lateral orbitofrontal	0	0.582941	0	2.533292	2.558164	0.358075
Medial orbitofrontal†	0	0.937806	0	2.291925	2.29459	0.921748
Paracentral	0	0	0.344678	2.303783	2.432269	3.63E-06
Pars opercularis	0	0	0.485284	2.508226	2.586642	0.001203
Pericalcarine†	0.707974	0	0	1.599123	1.645179	0.031204
Postcentral	0	0	0.294108	1.98767	2.11944	7.18E-10
Precentral	0	0	0.612908	2.456689	2.586754	1.56E-07
Precuneus	0.737268	0	0	2.336434	2.40409	0.004167
Rostral anterior cingulate	0	0.85751	0	2.757434	2.71241	0.258511
Rostral middle frontal	0	0.616103	0.431988	2.234575	2.276866	0.051859
Superior frontal†	0	0	0.431501	2.615406	2.682619	0.016246
Superior parietal†	0.822181	0	0	2.120708	2.217134	6.46E-06
Supramarginal	0.691152	0	0	2.511132	2.616694	5.58E-05
Frontal pole	0	0.67679	0	2.688236	2.698918	0.792354
Insula†	0	0.503879	0	2.987925	3.049985	0.026185

†Brain regions for which surface area, cortical thickness, and volume measurements of that region all contributed to subclassification.

**Table 4.—Loadings on Significant Volume MRI Features and the Mean Volume Measurements for the Two Subgroups**

Regions for Volume	Loadings		Means of MRI Features (mm <sup>3</sup> )		P Value
	Factor 1	Factor 2	Subgroup 1	Subgroup 2	
Caudal middle frontal	0.65666	0	5230.953	6364.619	9.98E-10
Cuneus†	0	0.626061	2674.094	2968.866	0.000205
Lateral occipital†	0	0.588881	10,154.66	11,689.81	7.47E-07
Lingual	0	0.783558	6364.472	6937.925	0.002633
Medial orbitofrontal†	0.670493	0	4254.462	4848.896	2.21E-07
Paracentral	0.84648	0	3195.906	3661.634	5.08E-08
Pars orbitalis	0	0.5658	2205.623	2439.052	0.000184
Pericalcarine†	0	0.724418	2012.802	2159.493	0.020236
Posterior cingulate	0.705502	0	2856.123	3319.321	2.84E-08
Rostral anterior cingulate	0.666202	0	2025.745	2373.522	3.67E-06
Superior frontal†	0.614916	0	18,895.27	21,963.5	9.15E-11
Superior parietal†	0	0.663085	11,605.25	13,616.74	4.08E-11
Supramarginal	0	0.588233	9533.849	11,222.27	4.14E-09
Insula†	0.564261	0	5934.83	6768.299	5.76E-10

†Brain regions for which surface area, cortical thickness, and volume measurements of that region all contributed to subclassification.

**Table 5.—Comparison of Migraine Subjects in Subgroup #1 vs Subgroup #2**

	Migraine: Subgroup #1 ( <i>n</i> = 34)	Migraine: Subgroup #2 ( <i>n</i> = 32)	<i>P</i> Value
Age in years (mean ± SD) ( <i>n</i> = 66)	37.3 ± 9.9	34.7 ± 12	.35
Sex (female:male) ( <i>n</i> = 66)	29:5	23:9	.23
Headache days/month (mean ± SD) ( <i>n</i> = 66)	9.6 ± 7.3	8.1 ± 4.9	.32
Years with migraine (mean ± SD) ( <i>n</i> = 66)	19.2 ± 11.3	13 ± 8.3	.01*
Migraine aura (yes/no) ( <i>n</i> = 60)	15/16	11/18	.45
MIDAS (mean ± SD) ( <i>n</i> = 66)	25 ± 22.9	15.7 ± 12.2	.04*
Allodynia during headache (mean ± SD) ( <i>n</i> = 66)	6.1 ± 5.3	3.6 ± 3.2	.03*
Allodynia between headaches (mean ± SD) ( <i>n</i> = 66)	1 ± 2.4	0.6 ± 1.7	.36
Hyperacusis (mean ± SD) ( <i>n</i> = 60)	7.5 ± 6	9.8 ± 7.3	.17
Photophobia (mean ± SD) ( <i>n</i> = 60)	2.2 ± 2.7	2.7 ± 2.3	.39
State anxiety (mean ± SD) ( <i>n</i> = 66)	27.3 ± 7.8	26.3 ± 6.3	.58
Trait anxiety (mean ± SD) ( <i>n</i> = 66)	32.5 ± 10.3	30.6 ± 7.2	.39
Beck Depression Inventory (mean ± SD) ( <i>n</i> = 66)	4.7 ± 4.6	3.6 ± 4	.30

Migraine subjects in subgroup #1 had a greater number of years with migraine, more migraine-related disability, and greater symptoms of allodynia during migraine attacks. Allodynia scores during and between headaches were calculated from the Allodynia Symptom Checklist 12. Anxiety scores were calculated from the State-Trait Anxiety Inventory. Hyperacusis scores were calculated from the Hyperacusis Questionnaire. Photophobia scores were derived from the Photosensitivity Assessment Questionnaire. MIDAS = migraine disability assessment scale; SD = standard deviation. \**P* < .05.

Features that differed between the subgroups included: allodynia symptom scores during migraine attacks ( $6.1 \pm 5.3$  vs  $3.6 \pm 3.2$ , *P* = .03), number of years with migraine ( $19.2 \pm 11.3$  vs  $13 \pm 8.3$  years, *P* = .013), and MIDAS scores ( $25 \pm 22.9$  vs  $15.7 \pm 12.2$ , *P* = .04) (Table 2). Thus, migraine subjects in subgroup #2 (the cluster that contained the majority of healthy control subjects) had less allodynia during migraine attacks, fewer years with migraine, and less migraine-related disability. There were not significant differences in headache frequency ( $9.6 \pm 7.3$  days per month vs  $8.1 \pm 4.9$  days per month, *P* = .32) or migraine aura status (48% with aura vs 38% with aura, *P* = .45) when comparing the migraine patients in subgroup #1 to those in

subgroup #2. There were also no differences between migraineurs in the two subgroups for age, sex, allodynia symptom severity between headaches, hyperacusis, photophobia, anxiety, and depression.

Healthy control subjects in subgroup #1 and subgroup #2 did not differ in their average age ( $34.7$  years  $\pm 10.9$  vs  $37.5$  years  $\pm 11.5$ , *P* = .40), sex (female 57.9 vs 80%, *P* = .11), state anxiety ( $23.7 \pm 5.4$  vs  $25.4 \pm 5.2$ , *P* = .29), trait anxiety ( $27.8 \pm 9.7$  vs  $29.3 \pm 6.8$ , *P* = .56), depression ( $2.6 \pm 5.9$  vs  $2.0 \pm 2.5$ , *P* = .67), hyperacusis ( $4.6 \pm 4.5$  vs  $3.5 \pm 2.5$ , *P* = .34), photophobia scores ( $0.63 \pm 0.89$  vs  $1.1 \pm 2.0$ , *P* = .19), or allodynia without headache scores ( $0.05 \pm 0.23$  vs  $0.14 \pm .43$ , *P* = .32).

While we adopted the two subgroup structure with the minimum BIC, we also checked the models with similar BICs but including different numbers of subgroups or latent factors. The models with different numbers of factors resulted in a very similar subgroup structure to the current result. The models with different numbers of subgroups revealed no better differentiation among healthy controls and migraine patients. Also, no significant differences in terms of patients' demographics and other clinical variables were found in the model with three subgroups.

## DISCUSSION

The main findings of this study were that an automated subclassification of migraine based upon brain structure identified two subgroups, with one subgroup having more years with migraine, more severe allodynia symptoms during migraine attacks, and greater migraine-related disability. Headache frequency and aura status were not significantly different between the two subgroups that were formed according to measurements of regional brain cortical thickness, volumes, and cortical surface area. Each subgroup contained healthy controls and people with migraine, indicating that simply having migraine was not associated with brain structural aberrations of a magnitude that led to clear differentiation of the migraine brain from the brains of healthy control subjects.

In this study, number of years with migraine was significantly different when comparing migraine patients within each of the two subgroups. This result is consistent with other research neuroimaging findings showing that the number of years with migraine is associated with brain structure and function.<sup>2,21,22</sup> For example, a migraine classifier consisting of resting-state functional connectivity MRI data was more accurate in classifying people with migraine who had longer disease durations (>14 years; 96.7% accuracy) versus those with shorter disease durations (14 or fewer years; 82.1% accuracy) (of note, many of the subjects in that study were also included in this study).<sup>2</sup> If one presumes that brain structure and function change as a result of recurrent migraine attacks, this finding is

easy to accept—in general, the longer a person has had migraine, the more attacks they have had, and the greater the brain changes. In support of the notion that recurrent migraine attacks alter brain function, a single longitudinal study of 19 migraine patients who had increasing headache activity over 6 weeks demonstrated correlations between changes in functional connectivity and the worsening clinical pattern.<sup>23</sup> However, it is not definitively known if brain structure changes are a result of recurrent migraine attacks or if the extent of brain structure abnormality correlates with age of onset for migraine—eg, the more abnormal brain structure is, the younger age of onset for migraine, and/or the younger brain is more susceptible to the effects of migraine. In this study, there were no differences in age amongst the patients in each of the two migraine subgroups. Although this lack of difference in age is reassuring that the differences in brain structure are not due to aging, it remains unclear if the differences reflect the number of years with migraine or the age of onset of migraine or a combination of both.

The severity of allodynia symptoms during migraine attacks was significantly different between the two migraine subgroups; one subgroup had mild symptoms while the other had moderate symptoms. Allodynia symptom severity was measured using the ASC-12, a questionnaire that collects information about thermal, mechanical static, and mechanical dynamic allodynia.<sup>11</sup> Several imaging studies have shown differences in brain structure and function that are associated with symptoms of allodynia during migraine attacks.<sup>24-27</sup> Moulton and colleagues demonstrated that interictal migraineurs who reported symptoms of allodynia during migraine attacks had pain-induced hypoactivation of the brainstem in the area of the nucleus cuneiformis compared to healthy controls, a finding that suggests inadequate pain inhibition leading to development of allodynia.<sup>24</sup> Another study demonstrated that compared to migraineurs who do not develop allodynia during migraine attacks, those who develop allodynia have greater painful heat-induced activation of middle frontal gyrus and secondary somatosensory cortex.<sup>27</sup> A resting state

functional connectivity study demonstrated atypical functional connectivity of the periaqueductal gray and nucleus cuneiformis with other pain processing brain regions in migraineurs, the strength of which positively correlated with the severity of allodynia symptoms during migraine attacks.<sup>25</sup> A study investigating brainstem structure demonstrated that migraineurs have smaller midbrain volumes compared to healthy controls and that there was a negative correlation between midbrain volume and severity of allodynia symptoms.<sup>26</sup> In addition, allodynia has also been identified as a risk factor for developing more frequent migraines and for inadequate response to migraine treatment.<sup>28,29</sup> This combination of study results showing the impact of allodynia on determining brain structure and function in people with migraine, in mediating migraine prognosis, and on modifying the likelihood of responding to migraine treatment, supports an argument that future diagnostic classification systems could subtype migraine according to the presence or severity of allodynia.

The extent of migraine-related disability was also different between the two migraine subgroups. Migraine subjects in subgroup #1 had severe migraine-related disability while those in subgroup #2 had moderate migraine-related disability. Disability could be a marker for the severity of migraine symptoms as well as the person's ability to cope with their migraine symptoms; those less able to cope with the symptoms would have greater migraine-related disability.<sup>30</sup> Since the migraine subjects in subgroup #1 had more severe migraine burden including number of years with migraine and symptoms of allodynia, it is expected that these patients would also have greater migraine-related disability. Independent of migraine severity, it is plausible that differences in the ability to cope with migraine could be associated with migraine-related disability and brain structural measures. Prior pain and migraine studies have identified associations between pain coping and catastrophizing with brain structure or function.<sup>31-34</sup> For example, an MRI study of migraineurs showed associations between pain catastrophizing with gray matter volume in primary somatosensory cortex, medial prefrontal

cortex, and anterior middle cingulate cortex and with cortical thickness in dorsolateral prefrontal cortex, middle temporal gyrus, and inferior frontal gyrus.<sup>31</sup>

The latent factors that differentiated subgroup #1 from subgroup #2 consisted of surface area, cortical thickness, and volume measurements of several different brain regions. These brain regions include those that are commonly implicated in different aspects of pain processing and many that have been previously identified to have structural or functional differences in people with migraine compared to healthy controls or in individuals who have migraine with allodynia compared to those who have migraine without allodynia.<sup>25,27,35</sup> For example, the anterior cingulate, insula, and somatosensory cortex, core regions of the 'pain matrix,' have frequently been identified as having atypical structure and function in people with migraine compared to healthy controls.<sup>36-38</sup> Several studies have identified multisensory regions, such as the temporal pole and regions near temporo-parietal and parieto-occipital junctions, to have structure and/or function that differs in the migraine brain compared to the healthy brain.<sup>3,39-41</sup> Atypical function of these regions that integrate somatosensory, visual, and auditory stimuli might contribute to the hypersensitivities associated with migraine and the exacerbation of headache via visual and auditory stimuli.<sup>42</sup> Frontal regions that contributed to migraine subclassification in this study likely participate in affective and cognitive components of pain processing, and many are regions previously identified as aberrant in migraine.<sup>43,44</sup> Compared to individuals who have migraine without allodynia, those who have migraine with allodynia have been shown in prior studies to have aberrant pain-induced activation of middle frontal gyrus and somatosensory cortex and altered functional connectivity with regions including the precuneus, middle and superior temporal gyri, middle and superior frontal gyri, and inferior and superior parietal gyri, all regions that contributed to migraine subclassification within this study.<sup>25,27</sup> Also, several regions that contributed to migraine subclassification in this study also contributed to

migraine classification models consisting of brain structure or function in previously published studies (many of the research participants in those studies were also included in the current study).<sup>2,4</sup> Those studies determined the accuracy for classifying individual patients as having episodic migraine versus chronic migraine versus being a healthy control using their imaging data, whereas this study used a data-driven approach to classify migraineurs into subgroups based solely on imaging data and then interrogated differences in clinical features between the individuals with migraine in each of the resulting subgroups.

Similar to our previous work using brain structure and function to classify migraine, the data-driven subgrouping of subjects in this study did not clearly distinguish people who have migraine from healthy controls.<sup>2,4</sup> This body of work suggests that not all people with migraine have brain structural or functional aberrations of a magnitude that allows for their separation from healthy non-migraine control subjects using MRI findings. The results from these classification studies suggest a logically plausible conclusion, that MRI classification of migraineurs is more accurate for those individuals who have a greater burden of disease. Taken together, these studies have shown that greater classification accuracy and automated subclassification are associated with more years with migraine, greater severity of allodynia during migraines, more migraine-related disability, and higher headache frequency.<sup>2,4</sup> Another possibility is that the timing of collecting MRI data unintentionally differs in participants with more severe migraine manifestations compared to those with less severe manifestations. Although all participants in these studies are considered “inter-ictal,” participants with more severe migraine manifestations might still have been closer to their next migraine attack and/or their last migraine attack and they might have more “inter-ictal” migraine symptoms such as inter-ictal hypersensitivities to stimuli. It has been demonstrated that migraine symptoms, functional MRI findings, and perhaps even structural MRI findings change as a person gets closer to and farther away from their last migraine attack.<sup>45-47</sup> Future studies should

consider this temporal relationship and they should explore if addition of other structural measures (eg, from diffusion tensor imaging) or functional measures (eg, functional connectivity) improve the ability of automated separation to distinguish individuals with migraine from healthy controls.

A limitation of this study includes the fact that two MRI scanners from different institutions were used to image the subjects. However, this was likely to have little impact on our results since nearly equal proportions of healthy control and migraine subjects were imaged on each of the two MRI scanners, there were no differences in total cortical volume ( $447,586 \text{ mm}^3 \pm 55,211$  vs  $457,494 \text{ mm}^3 \pm 57,342$ ,  $P = .35$ ) or total gray matter volume ( $604,513 \text{ mm}^3 \pm 69,680$  vs  $618,816 \pm 69,528 \text{ mm}^3$ ,  $P = .27$ ) when comparing images collected on the two scanners, and there was not an effect of the scanner used on the automated subgrouping of MRIs (62% of scans in subgroup #1 were performed on scanner #1 and 55% of scans in subgroup #2 were performed on scanner #1,  $P = .46$ ). In the future, tissue segmentation methods that are based on using both, T1 and T2 data might improve image postprocessing quality and could improve consistency of brain volume information when multiple scanners are used.<sup>48</sup> Another limitation is that we had missing data for migraine aura status, hyperacusis scores, and photophobia scores from six migraine subjects; thus, these specific data points were not available for our analyses. It is likely that these missing data had little impact on our overall study findings since three of these migraine subjects were categorized into subgroups #1 and 3 into subgroup #2. This study showed that a data-driven subclassification of brain MRIs divided the healthy controls into two subgroups. Amongst these healthy controls, there were not differences in measured variables such as age, sex, anxiety, and depression. These findings suggest that there were significant but unknown sources of variability associated with MRI structural features that were not measured during this study. Although the number of subjects included in this study is relatively large compared to other imaging studies, the sample size might not have been large enough to detect more subtle differences

in clinical features between subjects in subgroup #1 and subgroup #2. In addition to having significantly more years with migraine, greater migraine-related disability, and more symptoms of allodynia during migraine, subjects in subgroup #1 had nonsignificantly higher headache frequency and allodynia symptoms between headaches and were nonsignificantly more likely to have migraine with aura. It is possible that a larger sample size would result in these differences being significant. In this paper, we followed the original FMM paper by using BIC as a model selection criterion and validated it empirically with the MRI data.<sup>19</sup> We acknowledge that there is no universally accepted criterion to compare models with different number of subgroups. Other criteria such as Vuong-Lo-Mendell-Rubin test, and AIC could also be tried and the results could be cross-referenced. In addition, we applied MFMM on migraine patients only, but no subgroup structure was found, possibly due to the sample size. It will be useful to apply the MFMM method to investigate subgroups among migraine patients using a larger dataset. Based upon previously published literature, mean depression scores amongst the healthy control and migraine cohorts in this study were lower than expected. Since the presence of depression might be associated with alterations in brain structure, it cannot be determined if the imaging findings in this study would apply to individuals who have migraine and depression. Finally, the results of this study should be confirmed using a new and independent cohort(s) of subjects.

## CONCLUSIONS

In conclusion, automated separation of migraine subjects into two subgroups based upon brain structure reveals that the number of years with migraine, the severity of allodynia symptoms during migraine attacks, and the severity of migraine-related disability are important factors associated with structure-based subclassification. Since allodynia is also associated with migraine prognosis and response to treatment, future migraine classification systems could consider allodynia when classifying migraine into subtypes.

## STATEMENT OF AUTHORSHIP

### Category 1

#### (a) Conception and Design

Todd J. Schwedt, Bing Si, Jing Li, Teresa Wu, Catherine D. Chong

#### (b) Acquisition of Data

Todd J. Schwedt, Catherine D. Chong

#### (c) Analysis and Interpretation of Data

Todd J. Schwedt, Bing Si, Jing Li, Teresa Wu, Catherine D. Chong

### Category 2

#### (a) Drafting the Manuscript

Todd J. Schwedt, Bing Si, Jing Li, Teresa Wu, Catherine D. Chong

#### (b) Revising It for Intellectual Content

Todd J. Schwedt, Bing Si, Jing Li, Teresa Wu, Catherine D. Chong

### Category 3

#### (a) Final Approval of the Completed Manuscript

Todd J. Schwedt, Bing Si, Jing Li, Teresa Wu, Catherine D. Chong

## REFERENCES

1. Classification Committee of the International Headache Society. The International Classification of Headache Disorders, 3rd edition (beta version). *Cephalalgia*. 2013;33:629-808.
2. Chong CD, Gaw N, Fu Y, et al. Migraine classification using magnetic resonance imaging resting-state functional connectivity data. *Cephalalgia*. 2016; epub ahead of print.
3. Schwedt TJ, Berisha V, Chong CD. Temporal lobe cortical thickness correlations differentiate the migraine brain from the healthy brain. *PLoS One*. 2015;10:e0116687.
4. Schwedt TJ, Chong CD, Wu T, et al. Accurate classification of chronic migraine via brain magnetic resonance imaging. *Headache*. 2015;55:762-777.
5. Classification Committee of the International Headache Society. The International Classification of Headache Disorders: 2nd edition. *Cephalalgia*. 2004;24:9-160.

6. Beck AT, Steer RA, Brown GK. *Manual for Beck Depression Inventory II (BDI-II)*. San Antonio, TX: Psychology Corp; 1996.
7. Spielberger C, Gorsuch R. *State Trait Anxiety Inventory for Adults: sampler Set, Manual, Test, Scoring Key*. Redwood City, CA: Mind Garden; 1983.
8. Khalfa S, Dubal S, Veillet E, et al. Psychometric normalization of a hyperacusis questionnaire. *ORL J Otorhinolaryngol Relat Spec*. 2002;64:436-442.
9. Bossini L, Fagiolini A, Valdagno M, et al. Photosensitivity in panic disorder. *Depress Anxiety*. 2009;26:E34-E36.
10. Bossini L, Valdagno M, Padula L, De Capua A, Pacchierotti C, Castrogiovanni P. Sensibilità alla luce e psicopatologia: Validazione del Questionario per la Valutazione della Fotosensibilità (Q.V.F). *Med Psicosomatica*. 2006;51:167-176.
11. Lipton RB, Bigal ME, Ashina S, et al. Cutaneous allodynia in the migraine population. *Ann Neurol*. 2008;63:148-158.
12. Stewart WF, Lipton RB, Dowson AJ, et al. Development and testing of the Migraine Disability Assessment (MIDAS) Questionnaire to assess headache-related disability. *Neurology*. 2001;56:S20-S28.
13. Gronenschild EH, Habets P, Jacobs HI, et al. The effects of FreeSurfer version, workstation type, and Macintosh operating system version on anatomical volume and cortical thickness measurements. *PLoS One*. 2012;7:e38234.
14. Dale AM, Fischl B, Sereno MI. Cortical surface-based analysis. I. Segmentation and surface reconstruction. *Neuroimage*. 1999;9:179-194.
15. Fischl B, Liu A, Dale AM. Automated manifold surgery: Constructing geometrically accurate and topologically correct models of the human cerebral cortex. *IEEE Trans Med Imaging*. 2001;20:70-80.
16. Fischl B, Salat DH, Busa E, et al. Whole brain segmentation: Automated labeling of neuroanatomical structures in the human brain. *Neuron*. 2002;33:341-355.
17. Segonne F, Dale AM, Busa E, et al. A hybrid approach to the skull stripping problem in MRI. *Neuroimage*. 2004;22:1060-1075.
18. Dempster AP, Laird NM, Rubin DB. Maximum likelihood from incomplete data via Em algorithm. *J R Stat Soc B Methodol*. 1977;39:1-38.
19. Montanari A, Viroli C. Heteroscedastic factor mixture analysis. *Stat Model*. 2010;10:441-460.
20. Burnham KP, Anderson DR. Multimodel inference understanding AIC and BIC in model selection. *Sociol Methods Res*. 2004;33:261-304.
21. Chong CD, Schwedt TJ. Migraine affects white-matter tract integrity: A diffusion-tensor imaging study. *Cephalalgia*. 2015;35:1162-1171.
22. Jin C, Yuan K, Zhao L, et al. Structural and functional abnormalities in migraine patients without aura. *NMR Biomed*. 2013;26:58-64.
23. Zhao L, Liu J, Yan X, et al. Abnormal brain activity changes in patients with migraine: A short-term longitudinal study. *J Clin Neurol*. 2014;10:229-235.
24. Moulton EA, Burstein R, Tully S, et al. Interictal dysfunction of a brainstem descending modulatory center in migraine patients. *PLoS One*. 2008;3:e3799.
25. Schwedt TJ, Larson-Prior L, Coalson RS, et al. Allodynia and descending pain modulation in migraine: A resting state functional connectivity analysis. *Pain Med*. 2014;15:154-165.
26. Chong CD, Plasencia JD, Frakes DH, Schwedt TJ. Structural alterations of the brainstem in migraine. *NeuroImage: Clin*. 2016;13:223-227.
27. Russo A, Esposito F, Conte F, et al. Functional interictal changes of pain processing in migraine with ictal cutaneous allodynia. *Cephalalgia*. 2017;37:305-314.
28. Lipton RB, Munjal S, Buse DC, et al. Predicting inadequate response to acute migraine medication: Results from the American Migraine Prevalence and Prevention (AMPP) Study. *Headache*. 2016;56:1635-1648.
29. Louter MA, Bosker JE, van Oosterhout WP, et al. Cutaneous allodynia as a predictor of migraine chronification. *Brain*. 2013;136:3489-3496.
30. Ford S, Calhoun A, Kahn K, et al. Predictors of disability in migraineurs referred to a tertiary clinic: Neck pain, headache characteristics, and coping behaviors. *Headache*. 2008;48:523-528.
31. Hubbard CS, Khan SA, Keaser ML, et al. Altered brain structure and function correlate with disease severity and pain catastrophizing in migraine patients. *eNeuro*. 2014;1:e2014.
32. Rogachov A, Cheng JC, Erpelding N, et al. Regional brain signal variability: A novel indicator of pain sensitivity and coping. *Pain*. 2016;157:2483-2492.
33. Emmert K, Breimhorst M, Bauermann T, et al. Active pain coping is associated with the response in real-time fMRI neurofeedback during pain. *Brain Imaging Behav*. 2016; epub ahead of print.

34. Henderson LA, Akhter R, Youssef AM, et al. The effects of catastrophizing on central motor activity. *Eur J Pain*. 2016;20:639-651.
35. Schwedt TJ, Chiang CC, Chong CD, et al. Functional MRI of migraine. *Lancet Neurol*. 2015;14:81-91.
36. Hadjikhani N, Ward N, Boshyan J, et al. The missing link: Enhanced functional connectivity between amygdala and viscerosensitive cortex in migraine. *Cephalalgia*. 2013;33:1264-1268.
37. Russo A, Tessitore A, Esposito F, et al. Pain processing in patients with migraine: An event-related fMRI study during trigeminal nociceptive stimulation. *J Neurol*. 2012;259:1903-1912.
38. Schwedt TJ, Chong CD, Chiang CC, et al. Enhanced pain-induced activity of pain-processing regions in a case-control study of episodic migraine. *Cephalalgia*. 2014;34:947-958.
39. Liu J, Zhao L, Li G, et al. Hierarchical alteration of brain structural and functional networks in female migraine sufferers. *PLoS One*. 2012;7:e51250.
40. Moulton EA, Becerra L, Maleki N, et al. Painful heat reveals hyperexcitability of the temporal pole in interictal and ictal migraine States. *Cereb Cortex*. 2011;21:435-448.
41. Zhao L, Liu J, Dong X, et al. Alterations in regional homogeneity assessed by fMRI in patients with migraine without aura stratified by disease duration. *J Headache Pain*. 2013;14:85.
42. Schwedt TJ. Multisensory integration in migraine. *Curr Opin Neurol*. 2013;26:248-253.
43. Mickleborough MJ, Ekstrand C, Gould L, et al. Attentional network differences between migraineurs and non-migraine controls: fMRI evidence. *Brain Topogr*. 2016;29:419-428.
44. Schmitz N, Admiraal-Behloul F, Arkink EB, et al. Attack frequency and disease duration as indicators for brain damage in migraine. *Headache*. 2008;48:1044-1055.
45. Coppola G, Di Renzo A, Tinelli E, et al. Evidence for brain morphometric changes during the migraine cycle: A magnetic resonance-based morphometry study. *Cephalalgia*. 2015;35:783-791.
46. Maniyar FH, Sprenger T, Monteith T, et al. Brain activations in the premonitory phase of nitroglycerin-triggered migraine attacks. *Brain*. 2014;137:232-241.
47. Schulte LH, May A. The migraine generator revisited: Continuous scanning of the migraine cycle over 30 days and three spontaneous attacks. *Brain*. 2016;139:1987-1993.
48. Reig S, Sanchez-Gonzalez J, Arango C, et al. Assessment of the increase in variability when combining volumetric data from different scanners. *Hum Brain Mapp*. 2009;30:355-368.